Available online at www.sciencedirect.com
ScienceDirect
Physica B 387 (2007) 328–332
PHYSICA B
www.elsevier.com/locate/physb

The role of MFM signal in mark size measurement in probe-based magnetic recording on CoNi/Pt multilayers

Li Zhang[a,*], James A. Bain[b], Jian-Gang Zhu[b], Leon Abelmann[c], Takahiro Onoue[c]

[a]Department of Applied Physics, University of Electronic Science and Technology of China, Chengdu 610054, People's Republic of China
[b]Data Storage Systems Center, Department of Electrical and Computer Engineering, Carnegie Mellon University, Pittsburgh, PA 15213, USA
[c]Systems and Materials for Information Storage Group, MESA+ Research Institute, University of Twente, P.O. Box 217, 7500 AE Enschede, The Netherlands

Received 21 December 2005; received in revised form 16 April 2006; accepted 20 April 2006

Abstract

A method of heat-assisted magnetic recording (HAMR) potentially suitable for probe-based storage systems is characterized. Magnetic marks were formed by a scanning tunneling microscopy (STM)-based thermal magnetic mechanism on a perpendicular CoNi/Pt multilayered film. Magnetic force microscopy (MFM) was applied to display those marks. The MFM signal is dependent of the lift-height during MFM scanning: smaller lift-height leads to higher resolution of the MFM image and a double-peak signal line, while higher lift-height leads to lower resolution and a single-peak signal line. Theoretical calculation of the magnetic field from the mark was executed. It agrees well with experiments, and demonstrates the method of mark size measurement in perpendicular media: full-width half-maximum (FWHM) of the measured MFM signal.

PACS: 75.50.Ss; 85.70.−w; 07.79.−v

Keywords: High-density magnetic recording; Magnetic force microscopy (MFM); Lift-height in MFM scanning

1. Introduction

The super-paramagnetic effect that induces the thermal relaxation of recorded information [1] is a fundamental obstacle to increasing magnetic recording density. To achieve thermal stability of recorded information, increases in the coercivity and anisotropy of the recording medium are needed. This makes traditional recording more difficult because conventional heads cannot generate sufficient field to switch the magnetization of the bits in thermally stable media. To overcome this obstacle, heat-assisted magnetic recording (HAMR), has been proposed [2]. HAMR draws on concepts from traditional magneto-optical (MO) recording for the writing process, but is not restricted to optical read-back.

In addition to optical heating methods suggested by extensions of MO recording, another possible approach to HAMR is the use of field emission current from a sharp metallic tip for heating. This has the possibility of very high spatial resolution as scanning tunneling microscopes (STM), which have similar architectures, show atomic resolution in surface observation [3–5]. Nakamura et al. [6] demonstrated this writing method with an STM several years ago, and saw a mark size that increased with increasing voltage between the tip and the film. We have also demonstrated the process previously [7–9], but saw different results from them. For the sake of meaningful discussion, the size of those written marks must be measured accurately. In order to demonstrate the standard of mark size measurement in perpendicular media, we study the relationship of MFM signal and the lift-height in scanning in both experimental and theoretical approach.

2. Experiments

The recording medium in our work is a CoNi/Pt multilayered film. It is composed of 20 repeats of

*Corresponding author. Tel.: +86 13981908195; fax: +86 28 83201939.
E-mail address: zhangli_cmu2005@yahoo.com.cn (L. Zhang).

0921-4526/$ - see front matter © 2006 Elsevier B.V. All rights reserved.
doi:10.1016/j.physb.2006.04.028

$Co_{50}Ni_{50}$(0.55 nm)/Pt(0.89 nm) bilayers, bearing a total thickness of 28 nm. It is fabricated on a bare silicon substrate, with a 23 nm thick Pt seedlayer. We measure its perpendicular anisotropy $K_u = 3.0 \times 10^5\,J/m^3$, saturation magnetization $M_S = 430\,kA/m$, and coercivity $H_C = 398\,kA/m$ at room temperature in a Vibrating Sample Magnetometer (VSM). A Digital Instruments Dimension 3000 scanning probe microscope (SPM) was used for writing and imaging. It includes three operation modes: atomic force microscopy (AFM) was applied to scan the topographic features of the film, magnetic force microscopy (MFM) was used to image the magnetic domain structures, and STM was used for thermal writing. The film is heated locally by applying pulses of 5 V in amplitude and 500 ns in duration, with a rise time of 100 ns to the sample. No externally applied field was used in these experiments, although it will clearly be necessary in any recording system implementation of this method. Demagnetizing fields from the surrounding region of the material switch the magnetization of the heated area.

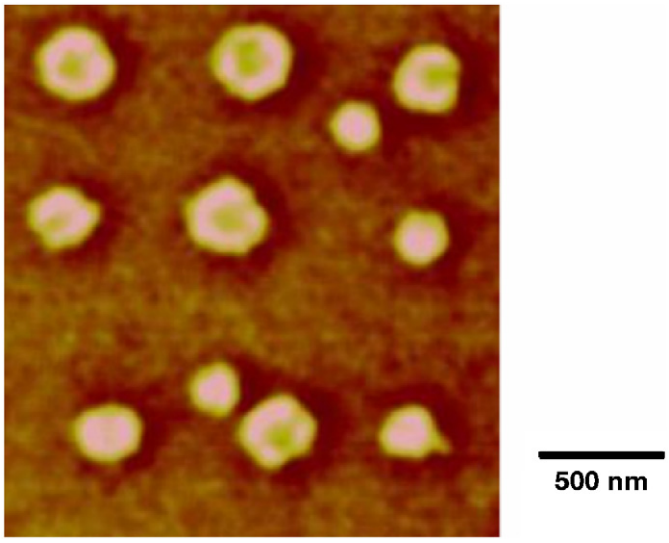

Fig. 1. MFM image of marks.

Fig. 1 shows some marks written on the film. In this figure, the MFM image was scanned with a lift-height of 10 nm. The role of lift-height in MFM is to delete the effect of atomic force [10]. In DI Dimension 3000 SPM, the MFM mode is operated together with AFM. Atomic force is a short-ranged force [11] while magnetic force is a long-ranged one [12]. By lifting the MFM tip away from the medium from the topographic scanning (AFM) to the magnetic scanning (MFM), the major portion of the atomic force will be eliminated in the MFM signal.

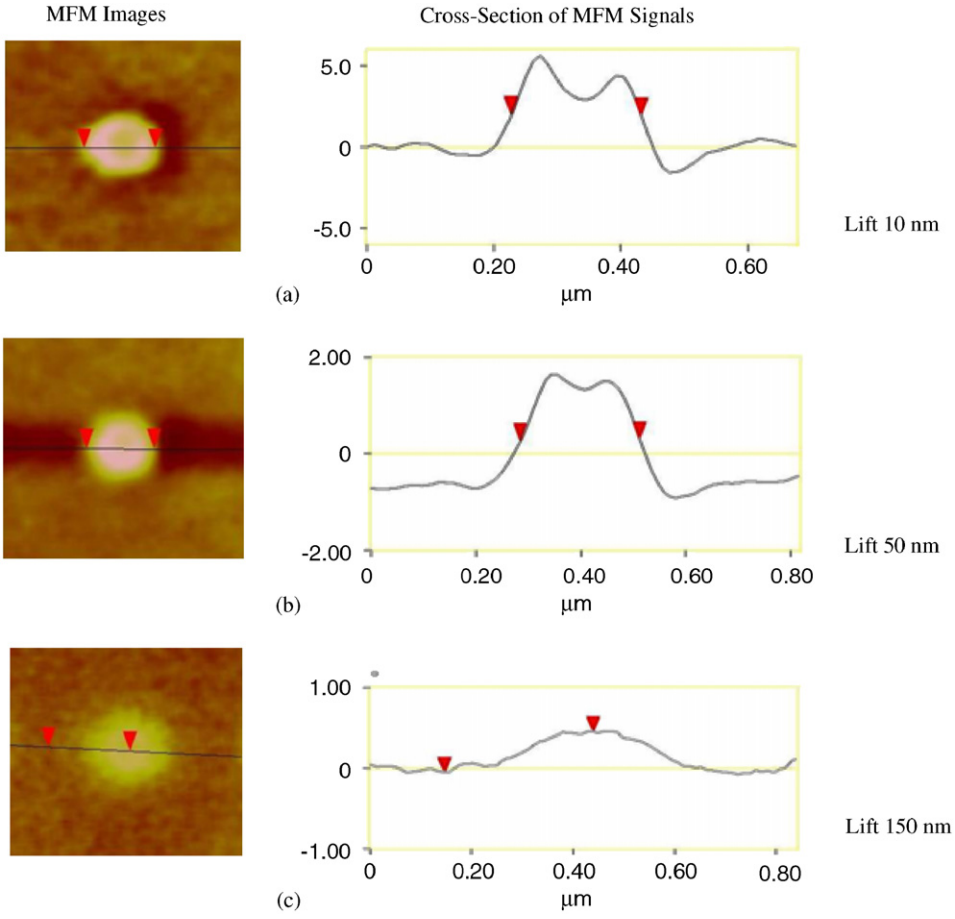

Fig. 2. MFM images and the cross-section of MFM signals of the same mark but in different lift heights.

A typical range of the lift-height is 10–200 nm. In the following steps, the lift-height is varied when the tip is scanning the same mark on the film. Fig. 2 shows a series of typical MFM images of the same magnetic mark but with different lift height. We see that the strength of the magnetic signal (i.e. the maximum MFM signal) decreases with increasing lift-height of the tip. In addition, the shape of MFM signal also changes: for small lift-heights, the MFM signal presents a distinct double-peak structure (Fig. 2a); with increasing lift-height, the double-peak structure blurs (Fig. 2b), and finally becomes a single-peak structure (Fig. 2c).

3. Models and discussion

In this section, we will study the mechanism of the MFM and the theoretical calculation of the MFM signal. MFM imaging is based on the magnetic field generated from the sample that is "sensed" by the tip. During imaging, we assume that the tip is uniformly magnetized in the direction along the tip's axis (Fig. 3), and its magnetization $\vec{M}$ is not affected by the stray field of the sample. In a simplified model, the actual size of the tip is neglected and it is treated as a dimensionless point. The magnetic medium generates a field, which surrounds the tip. The MFM signal is proportional to the magnetic force, or the field gradient $F_n \propto (\partial H_n/\partial n)$ [10]. For most regularly shaped magnetic domains, its magnetic field can be expressed analytically. We will be able to calculate the MFM signal analytically.

Next, let us calculate the magnetic field from the medium. Derived from Maxwell's Equations [12], the magnetic field generated by a magnet with a uniform magnetization $\vec{M}$ is

$$\vec{H}(r) = \frac{1}{4\pi}\iint \frac{\vec{M}(r')\cdot n'(r-r')}{|r-r'|^3}\,\mathrm{d}^2 r'. \tag{1}$$

In Eq. (1), r is the spatial position where the field on that point is to be solved, and r' is the position in the magnet and to be integrated. The surface integral in Eq. (1) varies with shapes of the magnet. In my work, the shape of thermally written mark is a circle in the film plane, and a cylinder in three-dimensional view. We describe it a cylindrical coordinate system, shown in Fig. 4. Because the marks are cylindrical, with the orientation of the magnetization along the central axis of the cylinder, Eq. (1) can be simplified due to the axial-symmetry of the system. Among the three coordinates (r, θ, z), r is the radial direction in the plane of the film, z is the direction normal to the film, and θ is the axial angle along the z-axis. Due to axial-symmetry, all the related physical parameters in this problem are θ-independent. Fig. 5 shows the illustration of the decomposition of a recorded bit with its surroundings, which is just a simple addition of a larger cylinder magnet with magnetization $+\vec{M}$ and a recorded bit (smaller cylinder magnet) with magnetization $-2\vec{M}$. Therefore, the key point of this problem is to calculate the magnetic field of a single uniform magnetic cylinder, with magnetization $\vec{M}$ along the center axis of the cylinder. From Eq. (1), the magnetic field from a single uniform magnetic cylinder can be expressed as:

$$\vec{H}(r,\theta,z) = \frac{M_0}{4\pi}\left\{\int_0^{2\pi}\mathrm{d}\theta'\int_0^a \frac{\vec{r}-\vec{r'}}{\left[(z-d)^2+\left(r\sin\theta-r'\sin\theta'\right)^2+\left(r\cos\theta-r'\cos\theta'\right)^2\right]^{3/2}} r'\,\mathrm{d}r' - \int_0^{2\pi}\mathrm{d}\theta'\int_0^a \frac{\vec{r}-\vec{r'}}{\left[(z+d)^2+\left(r\sin\theta-r'\sin\theta'\right)^2+\left(r\cos\theta-r'\cos\theta'\right)^2\right]^{3/2}} r'\,\mathrm{d}r'\right\} \tag{2}$$

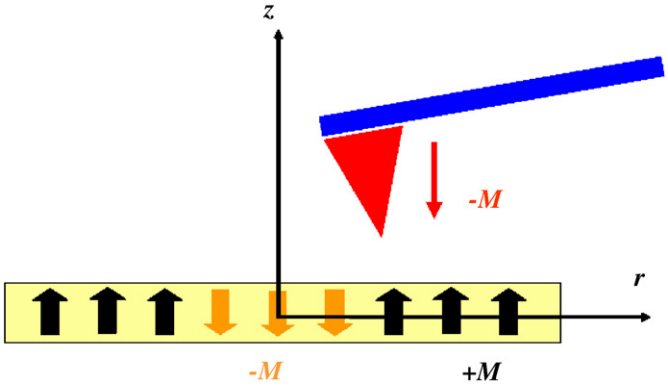

Fig. 3. Schematic diagram of an MFM tip in the field generated by the magnetic medium.

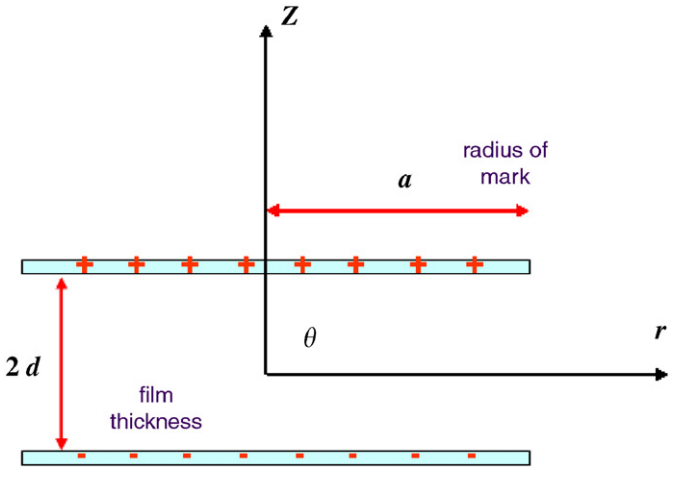

Fig. 4. Cylindrical coordinates to calculate magnetic field from a cylinder magnet.

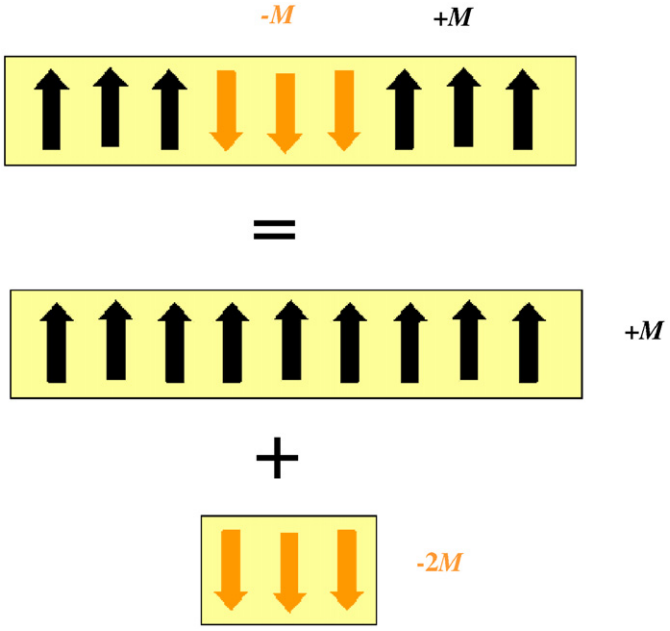

Fig. 5. Decomposition of a recorded bit to an addition of two uniform magnetic cylinders.

Where a is the radius of cylinder (or radius of mark), and $2d$ is the height of cylinder (or film thickness). The expression of three components of the field $\vec{H}(r,\theta,z)$, H_z, H_r and H_θ, can be achieved from Eq. (2). Due to axial-symmetry and the normal component of the MFM signal, we only study $H_z(r,z)$ in details. For the upper plate of the cylinder, $\overrightarrow{r} - \overrightarrow{r'} = (\sqrt{(r\cos\theta - r'\cos\theta')^2 + (r\sin\theta - r'\sin\theta')^2},\ \arctan(r\sin\theta - r'\sin\theta'/r\cos\theta - r'\cos\theta'),\ z-d)$, and similar expression as the lower plate. Thus we get

$$H_z(r,z) = \frac{M_0}{4\pi}\int_0^{2\pi} \mathrm{d}\theta' \times \int_0^a \left\{ \frac{z-d}{[(z-d)^2 + r'^2 - 2rr'\cos\theta' + r^2]^{3/2}} - \frac{z+d}{[(z+d)^2 + r'^2 - 2rr'\cos\theta' + r^2]^{3/2}} r'\,\mathrm{d}r' \right\}, \quad (3)$$

where we take $\theta = 0$ because H is identical for all kinds of angle θ. Because Eq. (3) is involved with elliptical integrations, they cannot be solved completely analytically. We solved it numerically in Matlab (version 6.5).

Now, let us calculate the MFM signal theoretically for comparison experiments. Based on Eq. (3) and the method of addition shown in Fig. 5, we will be able to obtain the field gradient, $f_n = f_z = \mathrm{d}H_z/\mathrm{d}z$ in the r–z plane. For a specific value of the lift height d_{lift}, the z-component is constant, the sum of half film thickness and lift height, $z = (1/2)d_{\mathrm{film}} + d_{\mathrm{lift}}$. The MFM signal turns to a function of field gradient vs. the radial position r, $f_n(r) = \mathrm{d}H_z(r,z)/\mathrm{d}z|_{z=(1/2)d_{\mathrm{film}}+d_{\mathrm{lift}}}$. Let us plot the field gradient as a function of radial position for different lift heights. In the following numerical calculation, we use numerical values for the mark as: film thickness 20 nm, and mark radius 100 nm (mark size 200 nm). We picked up three values of lift height, 5, 50, and 150 nm, respectively. The MFM signal as a function of the radial position, r, for all three lift-heights is plotted together in Fig. 6. Because of the much weaker signal strength for the large lift heights, the MFM signal of 50 nm lift-height is amplified by 10 times, and that of 150 nm lift height is amplified by 25 times. After amplification, they can be displayed in a reasonable scale together with the 5 nm lift-height signal. From the figure, we clearly see a double-peak symmetric structure for low lift-height case (5 nm and 50 nm), while it becomes a single-peak structure for high lift-height case (150 nm). It is consistent with the experimental results in Fig. 2. However, we find some discrepancy between experimental results and theory, especially for very small lift-height case. In theory, for very small lift-height, the field gradient is almost zero in the center of mark; while the experimental result shows that it is not close to zero (see Fig. 2a). It is due to the finite size of the MFM tip. In simulation, we simplified it as a dimensionless magnetic point. While for a real MFM tip, the size is 20–30 nm. When the characteristic length of the imaging feature is much larger than the tip size, the dimension of the tip can be neglected; otherwise, the shape of tip has to be taken into account. Despite that, our simulation agrees with experiments well.

In addition, we will be able to figure out the criterion of mark size measurement from the theoretical calculation. In Fig. 6, the mark size is known as 200 nm in diameter based on the selected calculation parameters. When linked to the point in the plot where $r = 100$ nm, it is the one where the amplitude of the signal reaches full-width half-maximum (FWHM). Therefore, it is reasonable to apply this standard of mark size measurement to any cylindrical marks written on a perpendicular recording medium.

Regarding the effect of the finite size of the actual MFM tip, it is a complicated problem. Some peer researchers applied a restoration technique to remove the tip dependence of the MFM image: Zhu et al. [13] models the tip as a half sphere, and Candocia et al. [14] models the tip as a cube. Their results show that the modeling of the finite tip size reduces the resolution of the MFM image, but does not hurt the mark size measurement. Therefore, our simplification is a good one for mark size measurement.

4. Conclusion

We have demonstrated a thermo-magnetic writing process using an STM on perpendicular CoNi/Pt multi-layered medium. The thermal-magnetically formed marks are imaged by MFM. The MFM signal of marks is dependent of the lift-height in MFM scanning: smaller lift-height leads to higher resolution of the MFM image and a double-peak signal line, while higher lift-height leads to lower resolution and a single-peak signal line. Theoretical calculation of the MFM signal proves the experiments, and the method of the measurement of mark size written in

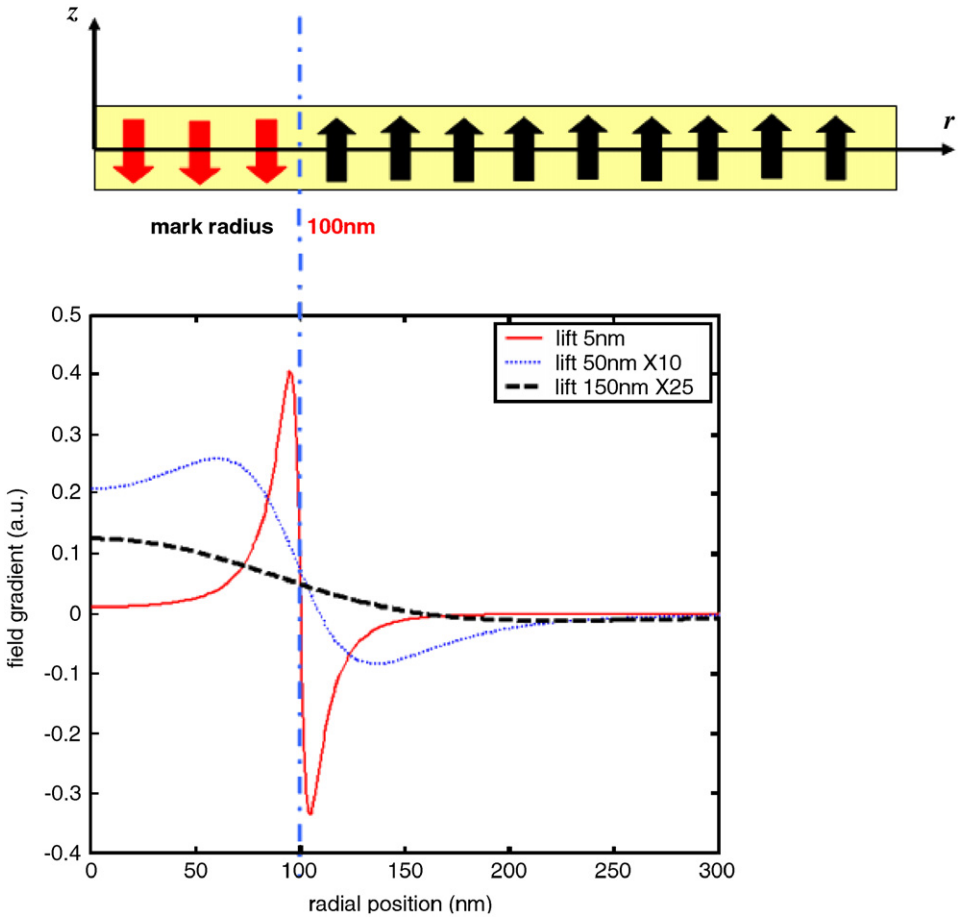

Fig. 6. Plots of the field gradient (MFM signal) as a function of MFM lift height.

perpendicular magnetic media: FWHM of the measured MFM signal.

Acknowledgments

This work is part of a project on MEMS-based magnetic mass storage systems [15] at the Center for Highly Integrated Information Processing and Storage Systems (CHIPS) in the Carnegie Mellon University, USA. This work was funded in part by NASA Grant ♯NAG8-1799.

Reference

[1] P.L. Lu, S.H. Charap, IEEE Trans. Magn. 31 (1995) 2767.
[2] J.J.M. Ruigrok, R. Coehoorn, S.R. Cumpson, H.W. Kesteren, J. Appl. Phys. 87 (2000) 5398.
[3] G. Binnig, H. Rohrer, Ch. Gerber, W. Weibel, Phys. Rev. Lett. 49 (1982) 57.
[4] G. Binnig, H. Rohrer, Ch. Gerber, W. Weibel, Appl. Phys. Lett. 40 (1982) 178.
[5] G. Binnig, H. Rohrer, Ch. Gerber, W. Weibel, Phys. Rev. Lett. 50 (1983) 120.
[6] J. Nakamura, M. Miyamoto, S. Hosaka, H. Koyanagi, J. Appl. Phys. 77 (1995) 779.
[7] L. Zhang, J.A. Bain, J.G. Zhu, L. Abelmann, T. Onoue, J. Appl. Phys. 99 (2006) 023902.
[8] L. Zhang, J.A. Bain, J.-G. Zhu, L. Abelmann, T. Onoue, J. Magn. Magn. Mater., 2006, in press.
[9] L. Zhang, J.A. Bain, J.-G. Zhu, L. Abelmann, T. Onoue, Phys. B 381 (2006) 204.
[10] S. Porthun, L. Abelmann, C. Lodder, J. Magn. Magn. Mater. 182 (1998) 238.
[11] G.A. Tsongas, S.P. Koutsoyannis, J. Phys. B (Atom. Mol. Phys.) Ser. 2 (1969) 437.
[12] J.D. Jackson, Classical Electrodynamics, 3rd edition, 1999
[13] J.-G. Zhu, X.D. Lin, R.C. Shi, Y.S. Luo, J. Appl. Phys. 83 (1998) 6223.
[14] F.M. Candocia, E.B. Svedberg, D. Litvinov, S. Khizroev, Nanotech 15 (2004) S575.
[15] L.R. Carley, J.A. Bain, G.K. Fetter, D.W. Greve, D.F. Guillou, M.S.L. Lu, T. Mukherjee, S. Santhanam, L. Abelmann, S. Min, J. Appl. Phys. 87 (2000) 6680.